DIRECT POLYNITROALIPHATIC ALCOHOL ADDITION TO ALKENES. 3. SYNTHESIS, STRUCTURE AND INTRAMOLECULAR ELECTRON IMPACT STABILITY OF THE UNIQUELY STRUCTURED 2,4-DIMETHYL-7,7-DINITRO-1,3,5-TRIOXACYCLOOCTANE

Raymond R. McGuire, [1] J. Lloyd Pflug, Margaret H. Rakowsky, Scott A. Shackelford,*[2] and Alan A. Shaffer[3]

Materials Chemistry Division, F. J. Seiler Research Laboratory (AFMC)
2354 Vandenberg Drive, Suite 2A35, USAF Academy, Colorado 80840-6272, U.S.A.

Abstract - Mercury(I) sulfate catalyzed addition between the difunctional 2,2-dinitropropane-1,3-diol (ADIOL) and the divinyl ether (DVE) diene reactants produces either an apparent acyclic acetal oligomer, or the unexpected eight-membered 2,4-dimethyl-7,7-dinitro-1,3,5-trioxacyclooctane. Proton nmr and deuterium labeling of this heterocyclic compound reveals it is comprised of both *meso* and *dl* diastereomers caused from its two chiral carbon atoms. Because this heterocycle incorporates both *gem*-2,2-dinitroalkyl and cyclic trioxane acetal structural fragments into one hybrid saturated ring structure, a novel intramolecular electron impact stability comparison can be made between the structural features representative of the normally unrelated geminal polynitroalkane and cyclic polyoxane compound classes which determine the fragmentation pathway of the subject heterocycle.

Recently reported was the high yield synthesis of new polynitroaliphatic acetal and ether products by a catalytic, non-alkaline, direct Markovnikov addition of 2-fluoro-2,2-dinitroethanol (FDNEOH) to various activated alkenes.[4] This mercury(I) or (II) sulfate catalyzed addition was especially interesting with the divinyl ether (DVE) isolated diene where the non-stereoselective diastereomeric diadducts (**1**) and monoadduct (**2**) could be preferentially obtained by varying the DVE/FDNEOH reactant stoichiometry. A minor competing transetherification reaction pathway gave a small amount of the 2-fluoro-2,2-dinitroethyl vinyl ether byproduct

(**3**) (Figure 1, Reaction A). In a subsequent article[5] it was shown that by changing to a mercury(II) oxide/trace trifluoroacetic acid co-catalyst, transetherification of divinyl ether with 2-fluoro-2,2-dinitroethanol becomes the major reaction pathway giving the vinyl ether product (**3**) (Figure 1, Reaction B). Here, the minor products also are a nearly equal mixture of the *meso*- and *dl*-diacetal products which are the major products in reaction A, Figure 1. Addition and transetherification both are occurring in reactions A and B, Figure 1; the one which predominates is determined by the catalyst used.

When extending this reaction with the non-conjugated divinyl ether diene (**4**) and the difunctional 2,2-dinitropropane-1,3-diol (**5**) reactants, stoichiometric variation of (**4**) and (**5**) produces another type of product control where either an apparent vinyl-terminated acyclic *gem*-dinitroaliphatic acetal oligomer (**6**) or the eight-membered 2,4-dimethyl-7,7-dinitro-1,3,5-trioxacyclooctane (**7**) forms in good yield (Figure 2). Incorporation of the *gem*-2,2-dinitroalkyl and cyclic trioxane acetal structural features into the single heterocylic ring (**7**) uniquely permits mass spectral confirmation of what ionization potentials, resonance stabilization and Stevenson's Rule[6] might predict concerning the relative electron impact decomposition stability of these two very different structural features which cannot be compared in separate unrelated compounds (Figure 3). The dashed line in Figure 3 provides a demarkation between these disparate structural features in (**7**) and readily compares the structures of compounds (**5**), (**7**), and (**8**). Described herein is the synthesis, structural characterization and electron impact stability determination of the novel 2,2-dimethyl-7,7-dinitro-1,3,5-trioxacyclooctane heterocycle (**7**) and its smaller six-membered heterocyclic analogue (**9**) which also contains this unique hybrid-type ring composition.

RESULTS AND DISCUSSION

Excess divinyl ether (**4**) reacted with the difunctional 2,2-dinitropropane-1,3-diol (**5**) in refluxing CH_2Cl_2 with mercury(I) sulfate catalyst produces a number of successive Markovnikov-directed additions and forms an apparent acyclic, vinyl-terminated acetal oligomer (**6**). Attempts to synthesize an analogous hydroxyl-terminated oligomer by reacting stoichiometric or excess (**5**) with the diene (**4**) in refluxing CH_2Cl_2 and mercury(I) sulfate catalyst produces instead an intramolecular Markovnikov-directed cyclization and forms the eight-membered, heterocyclic 2,4-dimethyl-7,7-dinitro-1,3,5-trioxacyclooctane (**7**) (48% isolated prior to distillation). The 2,4-dimethyl-7,7-dinitro-1,3,5-trioxacyclooctane (**7**) is a low melting opaque solid (mp

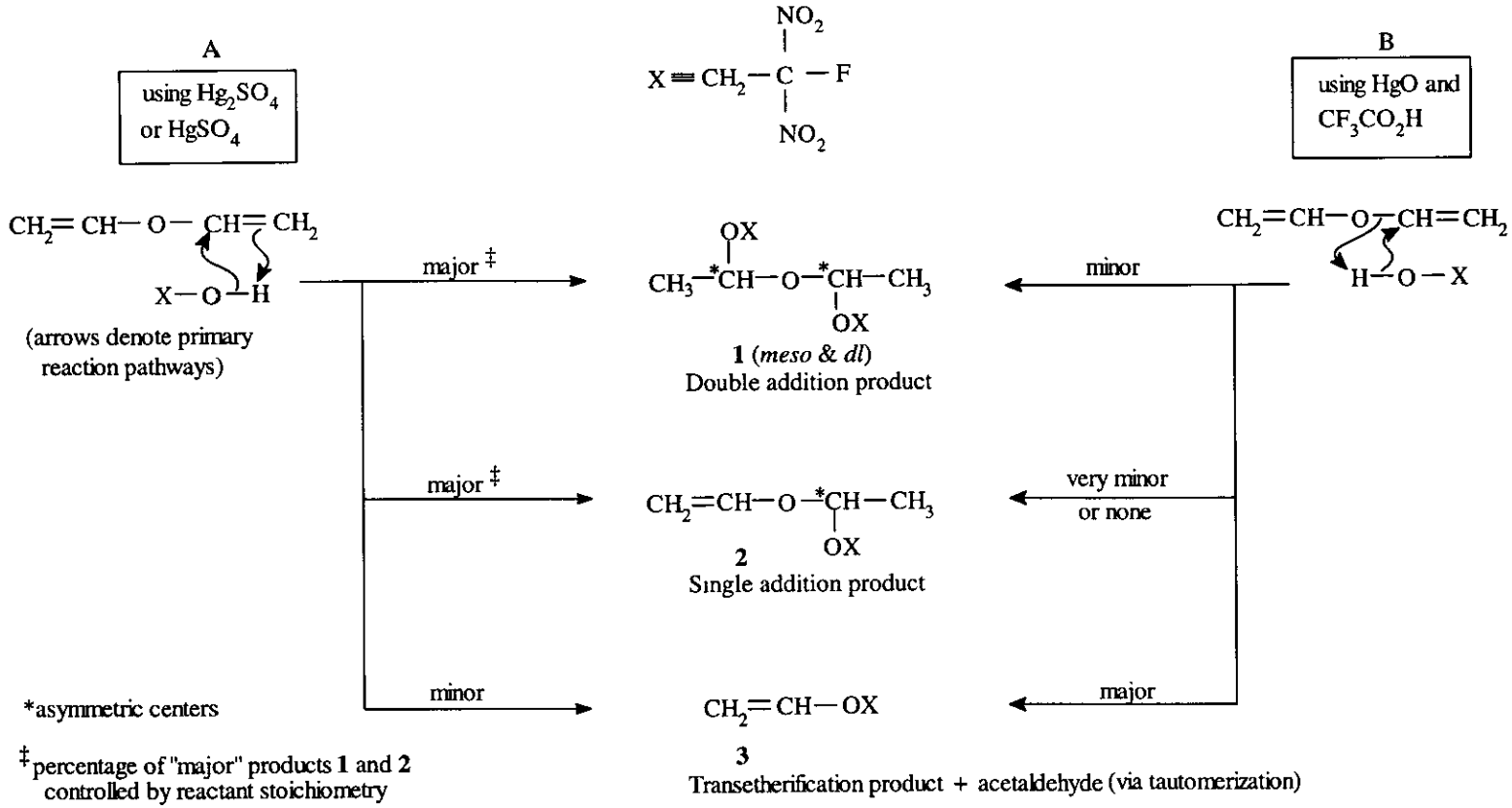

Comparison of reaction pathways

Figure 1

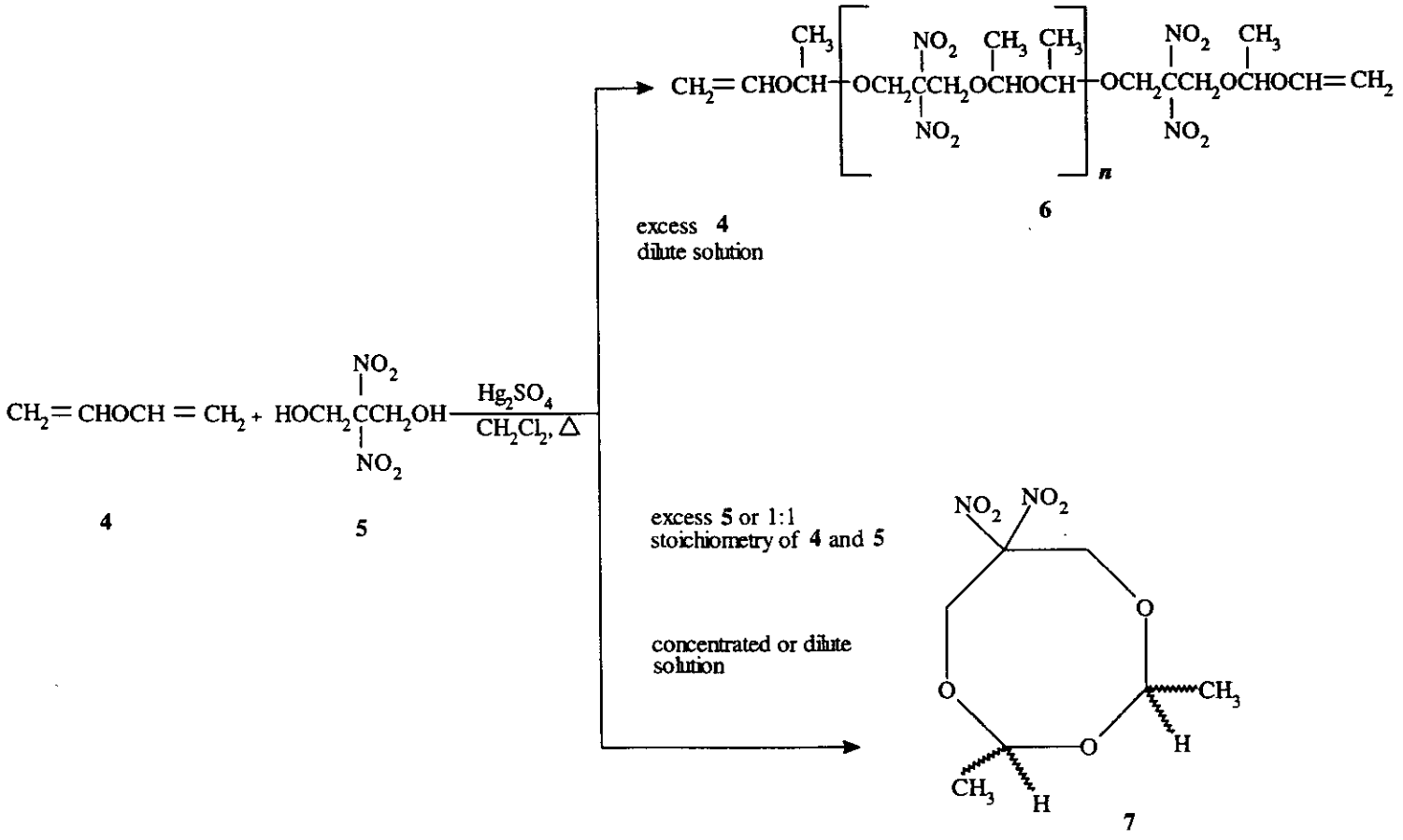

Reaction of (**4**) and (**5**) to form either oligomer (**6**) or heterocycle (**7**)

Figure 2

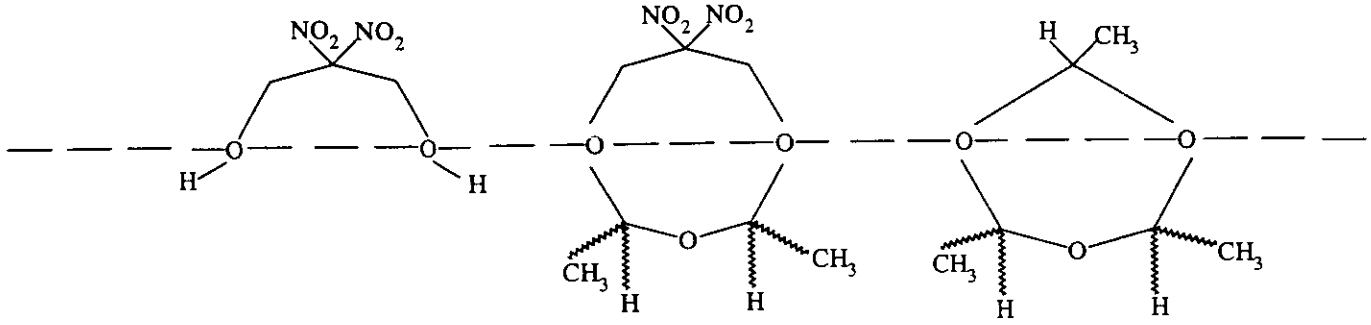

5

gem — dinitroalkane

7

8

cyclic acetal

Chemical structure comparison of compound (7) with compounds (5) and (8)

Figure 3

HETEROCYCLES, Vol. 38, No. 9, 1994

1983

54.2-56.8°C) and represents the first cyclic compound synthesized by this direct polynitroaliphatic alcohol addition reaction (Method 1 in Experimental Section). This new heterocycle (**7**) was characterized by proton nmr, infrared, high resolution mass spectrometry and carbon, hydrogen, nitrogen elemental analyses. This initial synthesis of (**7**) was conducted using a seven-fold excess of reactant (**5**), and because this initial synthesis of (**7**) was achieved prior to the availability for a gc/mass spectral analysis, the presence of any possible byproduct, such as (**9**), was below the detection limit of the instrumentation used in its identification. Figure 2 illustrates these two reaction pathways.

The apparent acyclic acetal oligomer (**6**) is a clear yellow oil with an average number of repeating structural units, n, ranging from 5 to 16 depending upon the reactant stoichiometry. The reaction described in the Experimental Section produces oligomer (**6**) with an average molecular weight of 4058 g/mol (n=16 units) and measured density of 1.32 g/ml. The value of n is estimated from proton nmr analysis using the integration value of two overlapping double doublets, presumed to be the terminal -OC<u>H</u>=CH_2 group's single vinyl proton. Noteworthy is the fact that the eight-membered heterocycle (**7**) can form from this oligomer (**6**) by an apparent thermally initiated decomposition which is followed by an immediate intramolecular cyclization. During an attempted and unsuccessful high temperature vacuum distillation of oligomer (**6**), an opaque solid, which proved to be compound (**7**), condensed on the molecular still's cold finger.

Later experiments using stoichiometrically equivalent amounts of divinyl ether and 2,2-dinitropropane-1,3-diol also gave in 45-55% overall crude yield after chromatography the cyclic product (**7**) which consists of the two *meso* and *dl* diastereomers, plus a small amount of a six-membered ring acetal byproduct, 2-methyl-5,5-dinitro-1,3-dioxacyclohexane (**9**) (Method 2 in Experimental Section). (These structural assignments were made based on ^1H nmr analysis and will be discussed subsequently). Attempted separation of the *meso* and *dl* isomers using a 60 cm capillary gas chromatography column was successful, with the six-membered ring acetal byproduct also appearing as a separate peak. When using a 10-fold dilution with CH_2Cl_2 solvent, a modest increase in this product mixture yield (62.5%) was obtained. These results indicate a direct intramolecular cyclization pathway to compound (**7**) when using the 1:1 stoichiometry. This diastereomeric product mixture is consistent with observations made from references 4 and 5. Because the monofunctional 2-fluoro-2,2-dinitroethanol (FDNEOH) adds twice to divinyl ether with the mercury(I) sulfate catalyst in

dichloromethane to provide a near equal mixture of the *meso*- and *dl*-diacetal compounds (Reaction A in Figure 1), one might expect to observe these isomers when (**5**) adds twice intramolecularly to the same reactive site in (**4**) using the same mercury(I) sulfate catalyst and the dichloromethane solvent. Also, because the transetherification reaction was a minor competing reaction pathway in the double addition of a monofunctional polynitroaliphatic alcohol (FDNEOH) to (**4**) (Reaction A in Figure 1), one might expect it to appear as a minor competing pathway when (**5**) reacts with (**4**). Figure 4 illustrates the 1:1 stoichiometric reaction of (**4**) and (**5**) where the eight-membered diastereomeric polynitroaliphatic trioxane (**7**) forms by the normal double addition when mercury(I) sulfate is used as the catalyst; however, formation of the minor six-membered cyclic dioxane analogue (**9**) also occurs by a minor competing reaction pathway. In this minor reaction pathway, a transetherification reaction apparently occurs in the first reaction step, which is then followed by the normal addition step expected when mercury(I) sulfate is the catalyst. The generally good yield of the entropically disfavored eight-membered cyclic trioxane (**7**) has some precedent in the literature.[7] Replacement of a methylene group by an oxygen atom is known to improve the formation of medium and large ring compounds and is credited to relief of unfavorable CH/CH repulsions. In this case, the presence of three oxygen atoms exaggerates this effect.

Two-proton spin-spin coupling patterns evident in the ^{1}H nmr of compound (**7**) are consistent with geminal splitting observed for equatorial and axial protons (Figure 5). Relative configurational assignment of the two chiral centers of compound (**7**) is possible based on the known deshielding of equatorial protons relative to axial protons. In a conformationally locked six-membered ring a chemical shift difference of equatorial versus axial protons of 0.1 to 0.7 ppm can be observed.[8] Although a rigid conformation is not present in the trioxacyclooctane structure, the presence of three oxygen heteroatoms within the cyclic array provides a comparable range of chemical shift differences, allowing a detailed analysis of splitting patterns in the ^{1}H nmr. Furthermore, the coupling constant (J) values observed for all geminal splitting patterns (≈13.3 Hz) fall within the 12-15 Hz range cited in reference 8. The complexity of the splitting pattern indicates approximately a 2:1 mixture of the two possible diastereomers, the *meso* and *dl* structures respectively, as well as the six-membered ring acetal byproduct compound (**9**), 2-methyl-5,5-dinitro-1,3-dioxacyclohexane (16.1% relative abundance by ^{1}H nmr integration). Figure 5 presents the ^{1}H nmr spectra of the diastereomeric product mixture of compound (**7**), an expanded region of the spectrum detailing the coupling

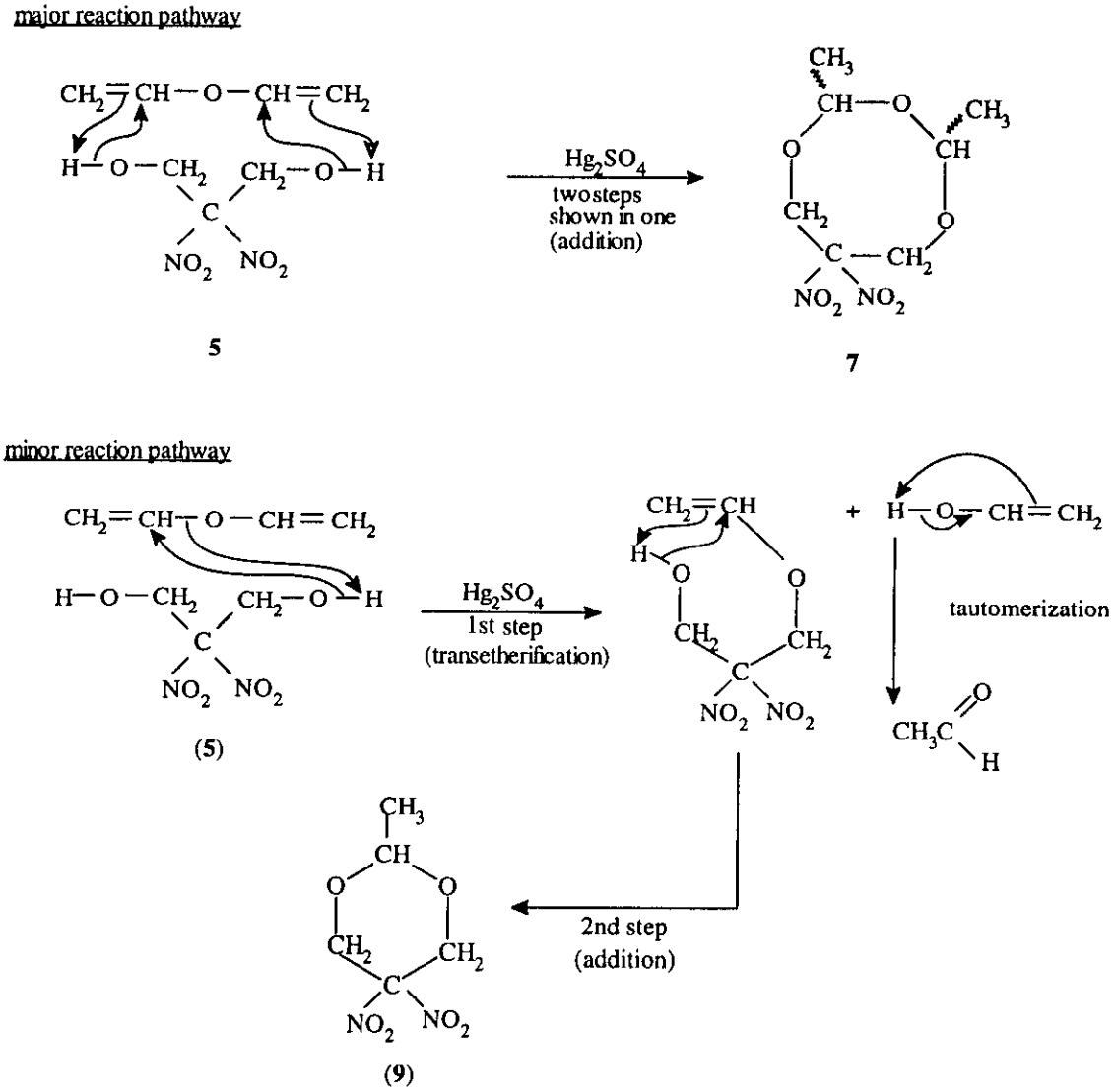

Competing reaction pathways using Hg_2SO_4 and difunctional substrates

Figure 4

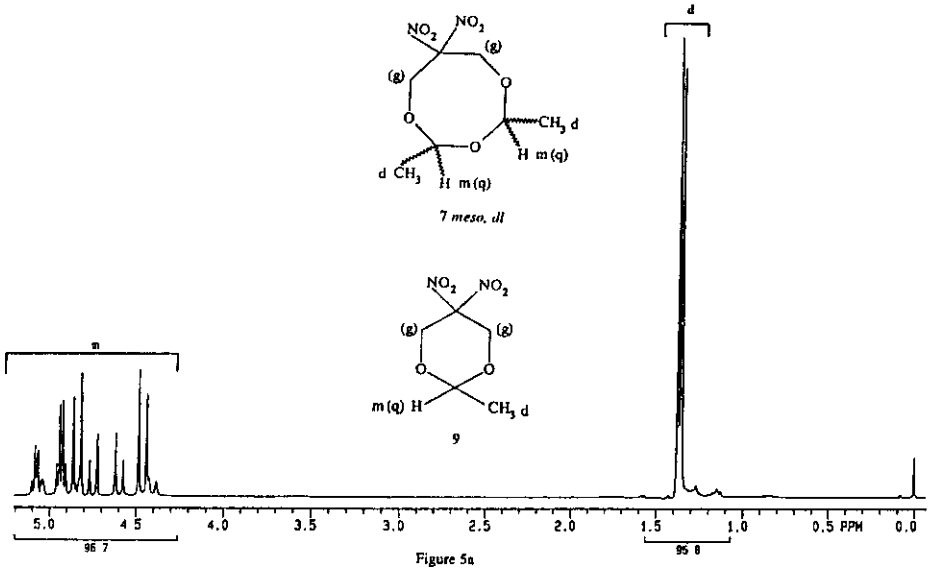

Figure 5a

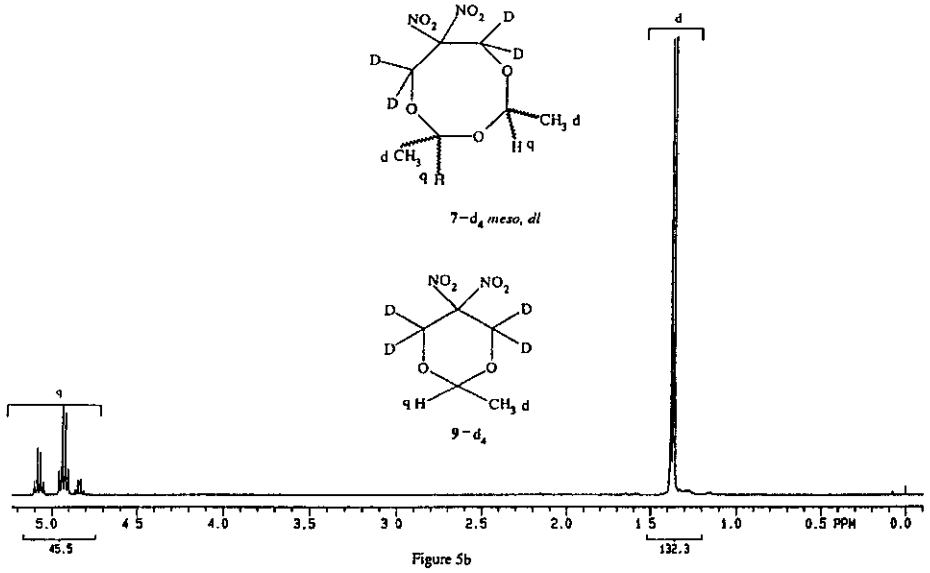

Figure 5b

Figure 5; 300 MHz ^{1}H nmr spectra of compound (**7**) and (**7**)-d_4 product mixture from Method 2, Experimental Section. Contains structures (**7**)-*meso*, (**7**)-*dl*, and (**9**), or the d_4 analogues respectively (see discussion).

(a) Overall spectrum of compound (**7**) product mixture showing doublet, d, and multiplet, m, patterns. Multiplet pattern contains geminal (g) and quartet (q) splittings shown with structures.

(b) Overall spectrum of compound (**7**)-d_4 product mixture. Geminal couplings are eliminated, leaving only quartet patterns.

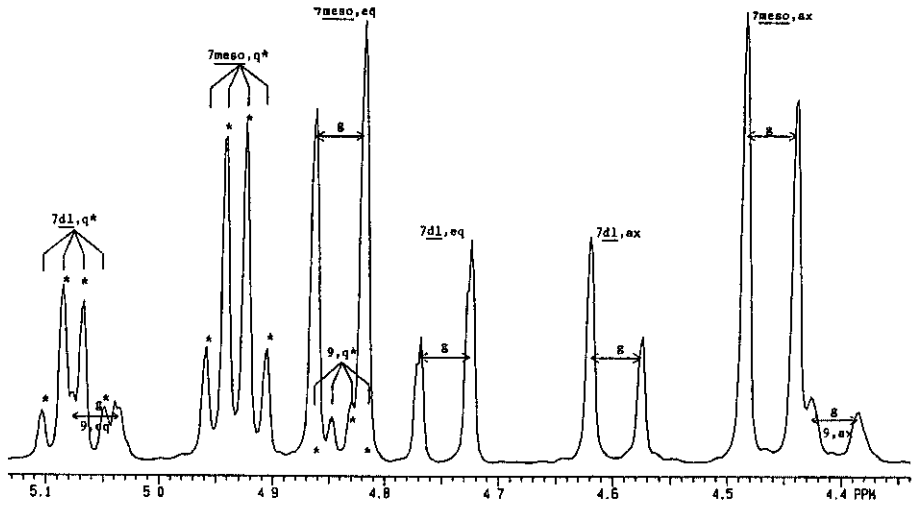

Figure 5c

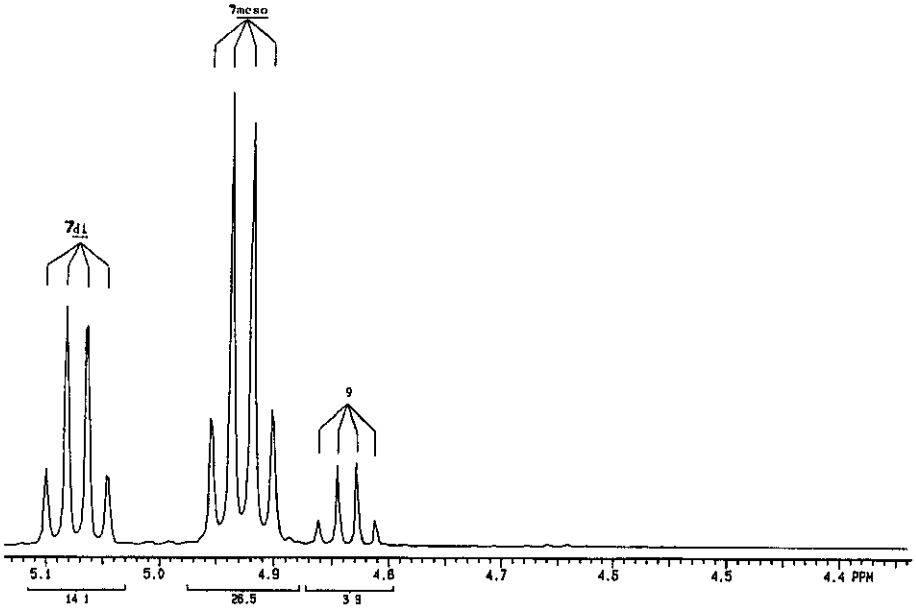

Figure 5d

Figure 5 continued

(c) Expanded multiplet pattern from Figure 5a; peaks identified by compound structure, (7)-*meso*, (7)-*dl*, or (9) and splitting pattern (g = geminal CH_2 splitting, eq = equatorial, ax = axial; q* = quartets identified by *). ↔ signifies J value for all geminal patterns = 13.3 Hz.

(d) Expanded region as in Figure 5c for compound (7)-d_4 product mixture showing relative integration values for quartet patterns identified by compound. Relative abundance of (7)-d_4 *meso*, (7)-d_4-*dl*, and (9)-d_4 are 54.8%, 29.1% and 16.1% respectively.

patterns, and the same spectra for the 6,6,8,8-tetradeutero substituted analogue, where all methylene group splitting from the geminal dinitroalkyl structural portion is removed. Observed peaks within the expanded region are identified by compound (Figure 5).

The *meso* diastereomer can be determined to be the predominant isomer for compound (**7**) using the relative intensities of the splitting patterns in the ^1H nmr. A greater relative deshielding of the diequatorial versus diaxial protons in the *meso* isomer versus the *dl* isomer is evident, because of the presence of the deshielding influence of two C-C sigma bonds (from the two methyl groups) located within the equatorial deshielding cone of the cyclic array of the *meso* isomer.[8] This should generate a greater difference in chemical shift of the equatorial versus axial protons for the *meso* versus *dl* isomer, consistent with the higher intensity splitting pattern bracketing the lower intensity splitting pattern. In the *dl* diastereomer, the time-average presence of only one methyl group in the deshielding equatorial cone generates a smaller chemical shift difference between the equatorial and axial CH_2 splittings (Figure 5). Cyclization favors formation of the *meso* isomer, whereas the acyclic isomer mixture (**1**) gave nearly the statistically expected 1:1 *meso* and *dl* diastereomeric ratio.[4] The predominant formation of the *meso* isomer in the cyclic structure (**7**) logically results from intramolecular steric product control favoring the more stable diequatorial (*meso*) methyl substitution pattern. In Figure 5, the greatest chemical shift difference is attributed to the comparable CH_2 geminal splittings of the 2-methyl-5,5-dinitro-1,3-dioxacyclohexane byproduct (**9**). The rigidity of the six-membered ring of this compound should accentuate the deshielding versus shielding of these protons. The lower intensity of these splittings also quantitatively correlates with the lower concentration of the byproduct. Integration of quartet patterns of CH-CH_3 for the (**7**)-d_4 product mixture indicates a relative concentration of this byproduct of ≈ 16%.

Without any further mass spectral mechanistic considerations, the unique incorporation of both a geminal dinitroalkane and an aliphatic cyclic acetal structural portion in heterocycle (**7**) provides an equal chance that the characteristic electron impact fragmentation process followed by either the 2,2-dinitroalkane or the cyclic trioxane acetal structural feature might occur. The predominance of a decomposition process in compound (**7**)'s hybrid chemical structure, which is characteristic of either a *gem*-2,2-dinitroalkane or an aliphatic trioxane acetal compound, would indicate which structural feature is the less stable toward an electron impact

decomposition process. This in turn should reflect the relative impact stability of the two usually unrelated geminal dinitroalkane and cyclic trioxane compound classes which cannot be compared separately. Validity of this comparative result, however, would depend upon the fact that the *gem*-dinitroalkyl and cyclic acetal structural features in compound (**7**) each display an electron impact initiated decomposition process which is similar to those characteristically followed by pure *gem*-2,2-dinitroalkanes and cyclic aliphatic acetal compounds.

While mass spectral studies of both pure nitroalkane and polynitroalkanes are limited,[9-12] the electron impact decomposition of 2,2-dinitropropane (DNP) is known.[11] Furthermore, its chemical structure closely resembles the *gem*-2,2-dinitropropyl structural feature comprising both compound (**7**) and reactant (**5**). Production of the *m/z* 30 $[NO]^+$ ion represents the predominant spectral feature (base peak) of both 2,2-dinitropropane and its 1,3-diol derivative (**5**).[13] Table I compares the loss of characteristic neutral or radical species for both DNP and (**5**) which produce their mass spectra. In the case of reactant (**5**), the identity of the possible neutral and radical fragments were also confirmed with the 2,2-dinitropropane-1,3-diol-1,1,3,3-d_4 ($HOCD_2C(NO_2)_2CD_2OH$) analogue (**5**-d_4).[13] These unlabeled DNP and *gem*-dinitroalkyl compounds such as (**5**) characteristically display ion masses involving loss of NO_2, NO, and OH radicals, plus HNO_2 and HNO neutral molecules during their mass spectral fragmentation.[13] Compound (**5**) also gives the CH_2O neutral fragment because of its inherent CH_2OH structural group. Cyclic alkyl-substituted aliphatic polyoxane acetals also often give no appreciable molecular ion but instead preferentially lose a pendant alkyl radical over a hydrogen atom and generate a resonance stabilized oxonium ion.[14,15] This oxonium ion normally forms at the carbon atom between two adjacent oxygen atoms in its ring.[15] The symmetrically substituted cyclic 2,4,6-trimethyl-1,3,5-trioxane acetal (**8**) provides an identical match with the cyclic aliphatic acetal structural feature which comprises a portion of the eight-membered heterocycle (**7**) (Figure 3). This analogous six-membered cyclic acetal (**8**) preferentially loses a methyl radical [$\bullet CH_3$] over a smaller amount of hydrogen atom [•H] in its initial fragmentation step. Further electron initiated decomposition provides the $CHOO^+$ (*m/z*=45) ion as its base peak, plus the CH_3CO^+ (*m/z*=43) ion as its second most abundant peak.[16]

Table I. Comparative Ion Masses and Possible Fragment Losses in 2,2-Dinitropropyl Compounds *

$CH_3C(NO_2)_2CH_3$(DNP)[11]		$HOCH_2C(NO_2)_2CH_2OH$(5)[13]		$HOCD_2C(NO_2)_2CD_2OH$ (5)-d_4[13]	
134	(a)	167	(b)	171	(c)(e)
[88](d)	$\bullet NO_2$	[121](d)	$\bullet NO_2$	125	$\bullet NO_2$
41	HNO_2	74	HNO_2	77	DNO_2
39	H_2	72	H_2	74	DH
		167	See Above	171	See Above
		149	H_2O	153	H_2O
		118	HNO	121	DNO
		72	$\bullet NO$	75	$\bullet NO_2$
134	See Above	149	See Above	153	See Above
88	$\bullet NO_2$	118	$\bullet CH_2OH$	120	$\bullet CD_2OH$
58	$\bullet NO$	149	See Above	153	See Above
43	$\bullet CH_3$	102	HNO_2	106	HNO_2
		72	$\bullet NO$	76	$\bullet NO$
(a) M+ apparently was		57	$\bullet CH_3$	59	$\bullet CD_2H$
not observed		149	See Above	153	See Above
		102	HNO_2	105	DNO_2
(b) M+1(H)=*m/z* 167		55	HNO_2	58	HNO_2
		149	See Above	153	See Above
(c) M+1(H)=*m/z* 171		31	$C(NO_2)_2{=}CH_2$	33	$C(NO_2)_2{=}CD_2$
		167	See Above	171	See Above
(d) Reference 11 shows no		137	HNO	139	DNO
m/z 88 ion from this		119	H_2O	122	$\bullet OH$
pathway; successive		102	$\bullet OH$	105	$\bullet OH$
loss of NO_2 and HNO_2		55	HNO_2	58	HNO_2
must be very rapid		137	See Above	139	See Above
since *m/z* 121 is		90	HNO_2	92	HNO_2
also not observed		60	CH_2O	60	CD_2O
for (5)		167	See Above	171	See Above
		136	$\bullet CH_2OH$	138	$\bullet CD_2OH$
(e) M+2(2H)=*m/z* 172		119	$\bullet OH$	121	$\bullet OH$
with 172-H_2O=*m/z* 154		89	$\bullet NO$	91	$\bullet NO$
and then 154-DNO=*m/z* 122		136	See Above	138	See Above
seen also in (5)-d_4		90	$\bullet NO_2$	92	$\bullet NO_2$
		119	See Above	121	See Above
		73	$\bullet NO_2$	75	$\bullet NO_2$
		118	See Above	121	See Above
		71	HNO_2	73	DNO_2
				171	See Above
				125	$\bullet NO_2$
				108	$\bullet OH$
				75	CD_2O
				108	See Above
				76	DNO
134	See Above				
88	$\bullet NO_2$				
71	$\bullet OH$				
41	$\bullet NO$				

* Note: Underlined masses are illustrated more than once in order to display the multiple fragmentation pathway of each.

Table II illustrates the mass spectral decomposition pathways followed by compound (**7**) and identifies the underlined ion masses which were determined by high resolution mass spectrometry. The more predominant *meso* isomer of the *meso/dl* diastereomeric mixture of (**7**) is illustrated; however, comparative examination of the *meso* and *dl* isomer mass spectrums (Figure 6) shows no significant differences. Additionally, the *m/z* ion masses and the fragment losses in Table II for compounds (**7**), (**9**), and (**10**) are consistent with deuterium atom incorporation observed in the ions generated from the mass spectra of the analogous deuterium-labeled (**7**)-d_4, (**9**)-d_4 and (**10**)-d_6 compounds respectively (Figure 7). While the ions and fragment losses seen in Table II are representative of both trioxanes and geminal dinitroalkanes, those characteristic of alkyl-substituted cyclic acetals like heterocycle (**8**)[14-16] predominate as the initially generated species during the electron impact decomposition of compound (**7**). This behavior may be explained by the relatively low ionization energy of trioxane compounds predicted by Stevenson's Rule[6] and by the initial formation of a resonance-stabilized oxonium ion (*m/z* 221) where the positive charge is delocalized over three atom centers (Figure 7).

The *m/z* 221 oxonium ion preferentially forms by loss of a pendant methyl radical instead of losing a hydrogen radical; this pattern is characteristic of methyl-substituted trioxanes.[14,15] Metastable peaks at *m/z* 168.5 and 141.5 establish the *m/z* 193 and *m/z* 177 ions as being daughter ions of the *m/z* 221 ion precursor, while another metastable at *m/z* 115 shows the *m/z* 149 ion is derived from the *m/z* 193 ion. The resonance stabilized *m/z* 177 oxonium ion represents the fourth most abundant peak for compound (**7**), which in turn spawns another oxonium ion at *m/z* 101 (Figure 7). Representing *m/z* 177 as an oxonium ion specie is further justified by the preferential generation of an identical *m/z* 177 oxonium ion from the six-membered heterocycle (**9**) by a homolytic cleavage of its pendant methyl group (Figure 7). The fragments seen for the higher ion masses during the initial part of the electron impact initiated decomposition of heterocycle (**7**) all are characteristic of those expected for cyclic methyl-substituted acetals. Except for the *m/z* 193 to *m/z* 146 fragmentation, only later in the decomposition pathway of (**7**) do fragments appear from lower mass ions which are characteristic of the *gem*-2,2-dinitroalkyl structure (Table II).

Table III lists the five most abundant mass spectral peaks generated by heterocycle (**7**). Three of these five ions are characteristic of cyclic trioxanes. Especially noteworthy are the CH_3CO^+ (*m/z* 43) base peak and the

Table II[a]. Electron Impact Fragmentation of Heterocycles (**7**), (**9**) and (**10**) *

meso-(**7**)			(**9**)			(**10**)		
m/z	(%)	Fragment loss	m/z	(%)	Fragment Loss	m/z	(%)	Fragment Loss
236	(0)	M^+				288	(10)	M^+
221	(5)	$\bullet CH_3$				231	(7)	$\bullet C(CH_3)_3$
193[b]	(9)	CO				175	(19)	$CH_2{=}C(CH_3)_2$
146	(2)	HNO_2				129	(9)	$\bullet NO_2$
86	(16)	CH_3CO_2H						
85	(10)	•H				288	(10)	See above
						273	(6)	$\bullet CH_3$
						242	(9)	HNO
221	(5)	See Above	192	(0)	M^+	224	(28)	H_2O
177[b]	(46)	CH_3CHO	177	(52)	$\bullet CH_3$			
131	(1)	$\bullet NO_2$	131	(2)	$\bullet NO_2$	273	(6)	See Above
101	(22)	•NO	101	(20)	•NO	217	(32)	$\bullet N{=}C(CH_3)_2$
57	(11)	CO_2	57	(17)	CO_2	171	(8)	$\bullet NO_2$
						115	(21)	$CH_2{=}C(CH_3)_2$
193	(9)	See Above	131	(2)	See Above	112	(20)	3 •H
149[b]	(12)	CH_3CHO	85	(12)	$\bullet NO_2$			
102	(7)	HNO_2				242	(9)	See Above
			192	(0)	See above	157	(13)	$CH_2{=}N{-}C(CH_3)_3$
146	(2)	See Above	146	(0)	$\bullet NO_2$	101	(19)	$CH_2{=}C(CH_3)_2$
116	(0)	•NO	116	(1)	•NO			
99	(4)	•OH	99	(6)	•OH	171	(8)	See Above
						143	(72)	$\bullet N{=}CH_2$
131	(1)	See Above	131	(2)	See Above			
102	(7)	•HCO	102	(15)	•HCO	143	(72)	See Above
						112	(20)	HNO
236	(0)	See above	192	(0)	See Above	288	(10)	See above
235[c]	(0)	•H	191	(4)	•H	287	(53)	•H
191	(5)	CH_3CHO	191	(4)	See above	287	(53)	See above
145	(4)	$\bullet NO_2$	145	(2)	$\bullet NO_2$	241	(12)	$\bullet NO_2$
115	(5)	•NO	115	(2)	•NO	224	(28)	•OH
87	(3)	CO	87	(2)	CO	241	(12)	See Above
145	(4)	See Above				195	(4)	$\bullet NO_2$
85	(10)	CH_3CO_2H						

* Note: Underlined masses determined by high resolution mass spectrometry.

a. Table II based on Gc/Mass Spectra taken for compounds (**7**), (**7**)-d_4, (**9**), (**9**)-d_4, (**10**), and (**10**)-d_6.

b. Successor ion determined from metastable specie in high resolution mass spectrum, i.e. *m/z* 193 from 221, *m/z* 177 from 221, and *m/z* 149 from 193. (see discussion)

c. Initial mass spectrum on a Dupont 21-491 double focusing instrument showed 0.4% peak at *m/z* 235.

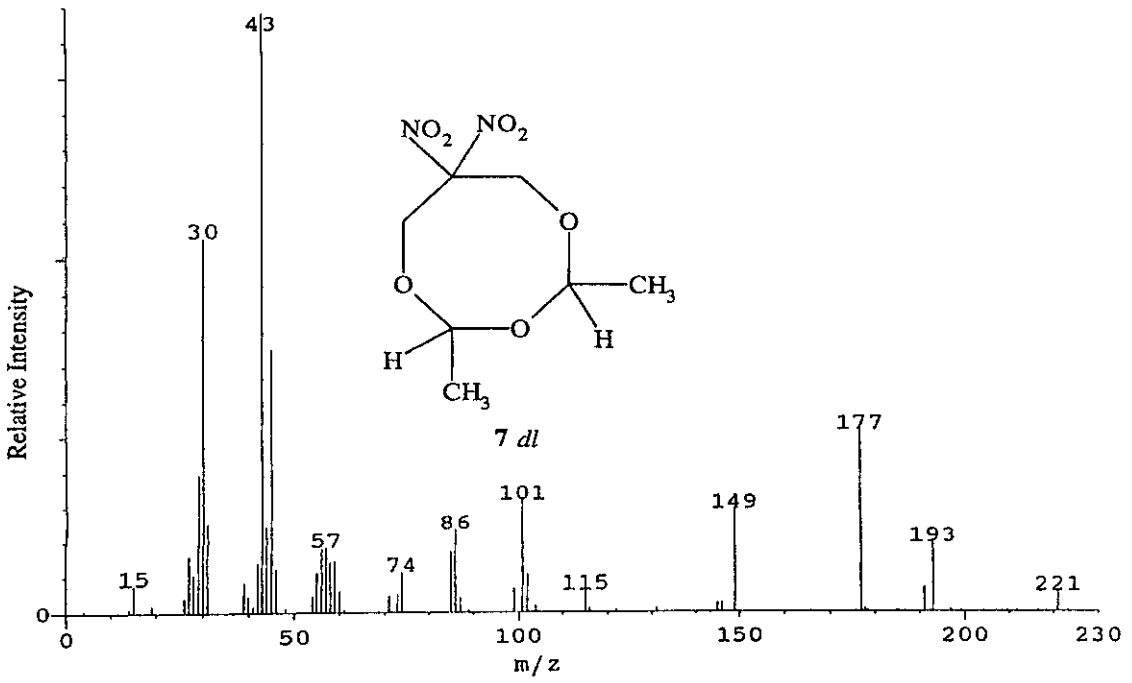

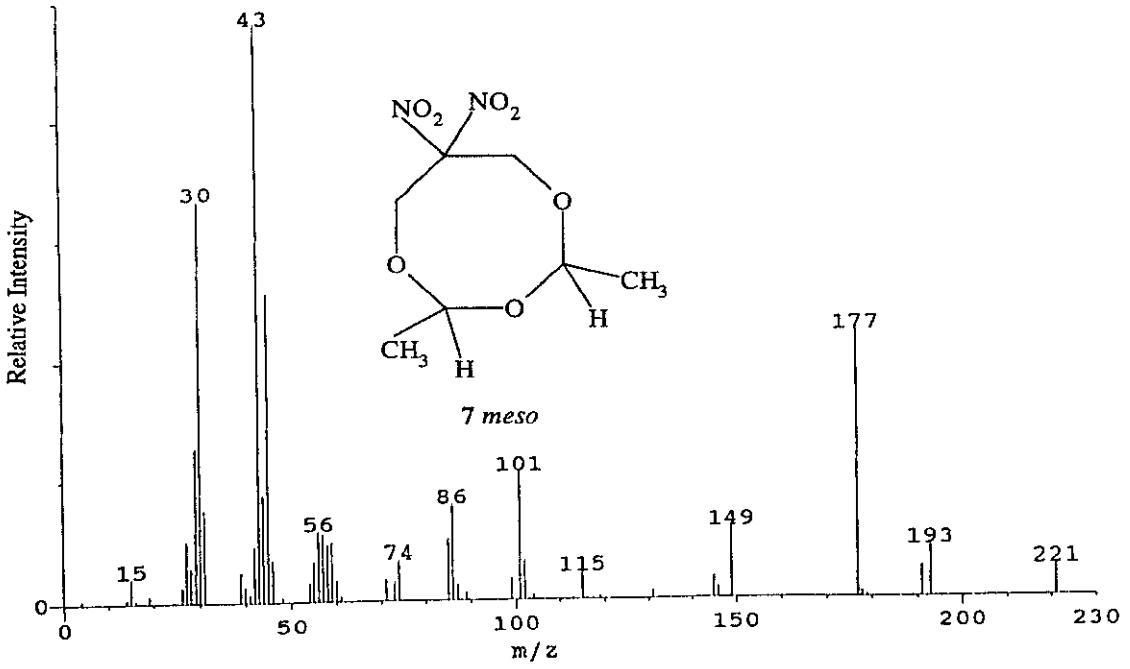

Mass Spectra of Product (7) Diastereomers
Figure 6

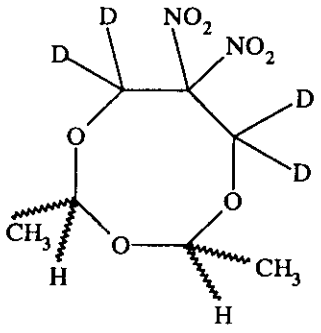

7 - d_4

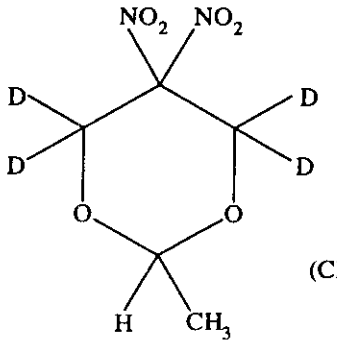

9 - d_4

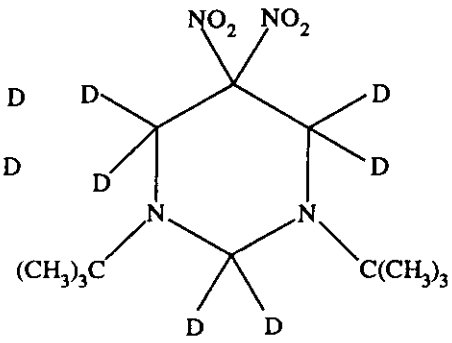

10 - d_6

a. Deuterium incorporation sites in (**7**)-d_4, (**9**)-d_4, and (**10**)-d_6

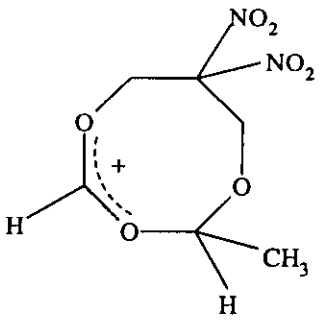

m/z 221

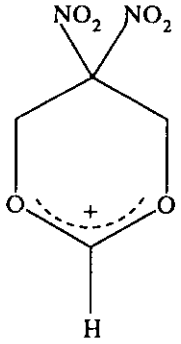

m/z 177

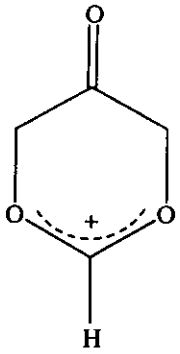

m/z 101

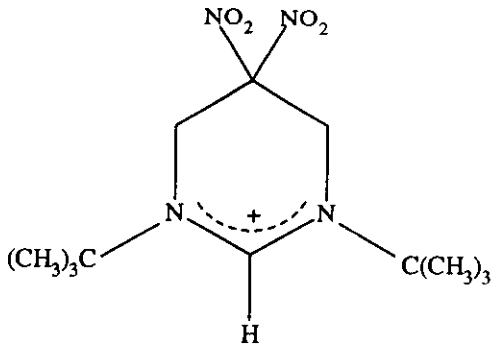

m/z 287

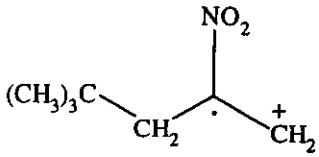

m/z 143

b. Key ion fragments derived from mass spectra of (**7**), (**9**), and (**10**)

Figure 7

Table III. Five Most Abundant Charged Ions of Heterocycles (**7**), (**9**) And (**10**)

	meso -(**7**)			(**9**)			(**10**)	
m/z	(%)	Charged Ion	*m/z*	(%)	Charged Ion	*m/z*	(%)	Charged Ion
43	(100)	CH_3CO	43	(100)	CH_3CO	57	(100)	$C(CH_3)_3$
30	(69)	NO, CH_2O	30	(89)	NO, CH_2O	143	(72)	Figure 7
45	(53)	HCO_2	177	(52)	Figure 7	287	(53)	Figure 7
177	(46)	Figure 7	45	(40)	HCO_2	41	(43)	$CH_2=CCH_3$
29	(26)	CHO	29	(26)	CHO	86	(33)	$CH_3NC(CH_3)_3$

Table IV. Low Molecular Weight Charged Ion Identification for Compound (**7**) And (**7**)-d_4

	meso-(**7**)				*dl* -(**7**)	
unlabeled	*m/z*	d_4		unlabeled	*m/z*	d_4
%		%	Charged Ion	%		%
26	29	6	HCO	23	29	5
69	30	91	CH_2O, NO, DCO	*63*	30	82
16	31	--	CH_2OH	15	31	--
--	32	*8*	CD_2O	--	32	*10*
--	33	27	CD_2OH	--	33	24

$CHOO^+$ (*m/z* 45) third most abundant ion; these two also are the most abundant charged species produced by the symmetrically-substituted cyclic 2,4,6-trimethyl-1,3,5-trioxane (**8**). The fourth most abundant *m/z* 177 oxonium ion produced by (**7**) has been discussed. The fifth most abundant ion is a CHO charged specie (*m/z* 29) which conceivably could be generated by either structural feature in (**7**)'s hybrid molecular structure. Only the second most abundant ion at *m/z* 30 might solely be characteristic of the *gem*-2,2-dinitroalkyl portion of the (**7**). Normally, the NO^+ (*m/z* 30) ion is the base peak generated by geminally-substituted 2,2-dinitroalkanes and their derivatives. But, the *m/z* 30 ion from compound (**7**) also could come in part from a charged CH_2O specie.

To examine this possibility, a detailed comparison was performed for the unlabeled and d_4 - labeled *meso* and *dl* diastereomers of compound (**7**). The following discussion refers to Table IV, where charged ion species for these structures have been identified in the center column. An *m/z* 32 abundance of 8% for the *meso*-(**7**)-d_4, compared to none for the *meso*-(**7**) unlabeled compound, suggests that about 8 units of the 69% abundance for the *m/z* 30 peak of the *meso*-(**7**), or 12%, comes from the CH_2O charged specie which then becomes the CD_2O ion for the *meso*-(**7**)-d_4 compound (See *meso*-(**7**) italicized entries in Table IV). The remaining *m/z* 30 abundance would come from the NO charged ion. The same reasoning for the *dl*-(**7**) unlabeled and d_4-labeled diastereomers suggests that 10 units of the 63% abundance for the *m/z* 30 peak, or 16%, comes from CH_2O with the remainder coming from the NO charged specie (See *dl*-(**7**) italicized entries in Table IV). Because the NO^+ is not the base peak for compound (**7**), and because its base peak is derived from the CH_3CO^+ (*m/z* 43) ion characteristic of symmetrically-substituted cyclic trioxanes, it appears the trioxane portion of compound (**7**) is less stable to an electron impact initiated decomposition process than is the geminal 2,2-dinitroalkyl component. Interestingly, except for a reversal of the third and fourth most abundant ions between (**7**) and its smaller six-membered analogue, (**9**), the five most abundant ions in their mass spectra are identical (Table III).

Mass spectral analysis of a cyclic six-membered di-*t*-butyl-substituted pyrimidine[13] (Figure 7) also suggests a higher relative electron impact stability for the *gem*-2,2-dinitroalkyl portion of a similar hybrid heterocyclic structure. The heterocycle, 1,3-di-*t*-butyl-5,5-dinitrohexahydropyrimidine (**10**), substitutes two ring nitrogen atoms for the oxygen atoms of the six-membered dioxane (**9**), and the pendant *t*-butyl groups are bonded to

the ring nitrogen atoms instead of the ring carbon atom located between the two ring oxygen atoms. Like (**7**) and (**9**), compound (**10**) also initially produces higher ion masses in its electron impact initiated decomposition pathway which are devoid of radical or neutral specie fragments characteristic of the geminal-2,2-dinitroalkyl structural portion. Of the five most abundant peaks produced in the mass spectrum of (**10**) (Table III), both the *m/z* 57 base peak and the *m/z* 41 charged species are derived exclusively from the pendant *t*-butyl group. The third most abundant peak at *m/z* 287 is a resonance-stabilized nitrogen analogue of heterocycle (**9**)'s *m/z* 191 oxonium ion, formed in the same manner by loss of a ring hydrogen radical (Figure 7). The second most abundant *m/z* 143 fragmentation initially involves only the pendant *t*-butyl group losing a methyl radical before the geminal 1,2-dinitroalkyl portion splits off an NO_2 radical. The fifth most abundant *m/z* 86 ion comes from both the cyclic pyrimidinyl and geminal 2,2-dinitroalkyl portions of the hybrid heterocyclic structure. Thus, four of the five most abundant charged species from (**10**) are either derived from the substituted cyclic pyrimidinyl structure of compound (**10**) or initially involve fragmentation of that structural portion. Note that none of these five most abundant species are the NO^+ (*m/z* 30) ion which characteristically is the base peak for geminal 2,2-dinitroalkanes.

It appears that the saturated cyclic acetal portion of the eight-membered heterocycle (**7**) structure, and its smaller six-membered analogue (**9**), intrinsically possess a lower electron impact stability than the geminal-2,2-dinitroalkyl portion of these two structurally hybrid molecules. This is demonstrated by (1) the predominant generation of radical and neutral fragments characteristic of saturated cyclic acetal compounds during the initial electron impact initiated decomposition pathway (Table II), (2) three of the five most abundant ions from (**7**) being produced from fragmentation pathways characteristically followed by substituted tri- and dioxanes, and (3) the selective generation of a base peak, *m/z* 43 from (**7**), which is characteristic of polyoxane molecules rather than the base peak, *m/z* 30, associated with *gem*-2,2-dinitroalkanes. This would suggest that cyclic polyoxane compounds as a class, likely are less stable to the mass spectral electron impact initiated decomposition process than is the 2,2-dinitroalkane compound class.

EXPERIMENTAL

General. The divinyl ether was purchased from PCR, Inc., Gainesville, FL, and initially was used without further purification. In later reactions, DVE was distilled over CaH_2 prior to use.[18,19] The initial 2,2-

dinitropropane-1,3-diol used was donated by the Naval Surface Warfare Center/White Oak Laboratory, Silver Spring, MD, and required no additional purification. (*CAUTION! The compound 2,2-dinitropropane-1,3-diol can be an explosive compound under the proper stimulus. Proper shielding and careful handling procedures should be used with this reagent.*) Nuclear magnetic resonance ^1H spectra were taken on a Varian Gemini 300 MHz instrument in $CDCl_3$ solvent (TMS internal reference). Infrared spectra were obtained as a thin film on a Beckmann IR-20 spectrophotometer with NaCl plates. Elemental analysis was performed by Galbraith Laboratories, Knoxville, TN. Mass spectra on compound (**7**) obtained by Method 1 was obtained with a Dupont 21-491 double focusing mass spectrometer using a direct insertion probe (DIP) at 78 eV ionizing voltage and a source temperature *ca.* 180° C; duplicate and high resolution mass spectral analyses on this sample were obtained at two other laboratories, AF Materials Laboratory (Analytical Services Branch), Los Alamos National Laboratory, and a third through the assistance of a Wright State University faculty member. The mass spectra data on compounds (**5**), (**5**)-d_4,(**7**), (**7**)-d_4 (Method 2), (**10**) and (**10**)-d_6 as seen in Tables I and II were obtained by DIP analysis with a Hewlett Packard 5985 Gc/Ms system.

Vinyl-terminated acetal oligomer (Product 6).

A 1000 ml single-necked round-bottom flask charged with 750 ml of CH_2Cl_2, 15.0 g (21.4 mmol) of divinyl ether (**4**), 11.85 g (7.1 mmol) of 2,2-dinitropropane-1,3-diol (**5**) and 2.9 g (5.8 mmol) of mercury(I) sulfate was stirred under reflux 118 h (5 days). Removal of CH_2Cl_2 by rotary evaporation gave 13.42 g of slightly yellow oil containing a solid suspension. The oil was poured onto a silica column which was prepared by placing into a 150 ml fritted glass medium porosity funnel, 25 g (60/200 mesh) silica gel powder slurried in CCl_4 with a 1/4 inch sand overlay. The oil was eluted through the silica gel column with 350 ml of CCl_4; rotary evaporation of the carbon tetrachloride produced 12.11g (78%) of a clear yellowish oil; ^1H nmr ($CDCl_3$) δ 6.40 and 6.34 (two overlapping dd, J=8 and 7 Hz, 2H) 4.76 (complex m, 53H), 1.36 (d, J=5 Hz, 51H); ir (cm^{-1}) 2980, 2940, 2890, 1645, 1630, 1570, 1320.

2,4-Dimethyl-7,7-dinitro-1,3,5-trioxacyclooctane (Product 7). (Method 1.)

A 50 ml single-necked round-bottom flask charged with 20 ml of CH_2Cl_2, 0.23 g (3.3 mmol) of divinyl ether (**4**), 3.50 g (21.1 mmol) of 2,2-dinitropropane-1,3-diol (**5**) and 550 mg (1.1 mmol) of mercury(I) sulfate was stirred under reflux 24 h. The reaction solution was filtered through a course glass sintered funnel; the

CH_2Cl_2 then was removed by rotary evaporation. The yellow tinted solid (much of it excess unreacted (**5**)) was coated onto alumina (pH 6.9) by dissolving this solid in acetone, adding 2.3 g of neutral alumina and removing the acetone solvent by rotary evaporation. The coated alumina was placed atop a 1.5 x 10.0 cm^2 silica gel column packed with CH_2Cl_2. Elution with CH_2Cl_2 and solvent removal by rotary evaporation gave 0.37 g (48%) of a light yellow oil. This oil was further purified by vacuum distillation at 70-71°C/0.25 mm Hg in a molecular still and afforded 0.21 g (27%) of a colorless oil that solidified in a refrigerator to a solid (mp 54.2-56.8°C); ^1H nmr ($CDCl_3$) δ 4.87 (m, 6H), 1.49 (d, J=5 Hz, 6H); ir (cm^{-1}) 2990, 2940, 2880, 1570, 1315; *Anal.* Calcd for $C_7H_{12}N_2O_7$: C, 35.6; H, 5.1; N, 11.9. Found: C, 35.4; H, 4.9; N, 12.0.

2,4-Dimethyl-7,7-dinitro-1,3,5-trioxacyclooctane (Product 7). (Method 2.)

A 50 ml single-necked round-bottom flask was charged with 20 ml of CH_2Cl_2, 0.23 g (3.3 mmol) of divinyl ether (**4**), 0.55 g (3.3 mmol) 2,2-dinitropropane-1,3-diol (**5**) and 550 mg (1.1 mmol) of mercury(I) sulfate and stirred under reflux 24 h. Workup in the manner of Method 1 gave a light yellow oil. Chromatography (Method 1) gave a colorless oil which solidified upon cooling to give 0.367 g of product (47.1%). A confirmatory ^1H nmr spectrum is shown in Figure 5a. Reaction on the same stoichiometric scale but using 200 ml CH_2Cl_2 solvent gave a 62.5% yield of isolated product. Use of 1,1,3,3-tetradeutero-2,2-dinitropropane-1,3-diol starting material[13] gave the 6,6,8,8-tetradeutero-2,4-dimethyl-7,7-dinitro-1,3,5-trioxacyclooctane product in comparable yield. A confirmatory ^1H nmr spectra is shown in Figure 5b. Ms of *meso*-(**7**) [*m/z* (%)]: 221 (5), 193 (9), 191 (5), 177 (46), 149 (12), 145 (4), 115 (5), 102 (7), 101 (22), 99 (4), 87 (3), 86 (16), 85 (10), 74 (7), 73 (3), 71 (4), 60 (4), 59 (10), 58 (10), 57 (11), 56 (12), 55 (7), 54 (3), 46 (7), 45 (53), 44 (18), 43 (100), 42 (9), 40 (3), 39 (5), 31 (16), 30 (69), 29 (26); Ms of *dl*-(**7**): 221 (3), 193 (11), 191 (4), 177 (31), 149 (17), 115 (3), 102 (6), 101 (19), 99 (4), 86 (14), 85 (10), 74 (7), 73 (3), 71 (3), 60 (4), 59 (8), 58 (8), 57 (11), 56 (11), 55 (7), 54 (3), 46 (7), 45 (44), 44 (14), 43 (100), 42 (8), 40 (3), 39 (5), 31 (15), 30 (63), 29 (23); Ms of *meso*-(**7**)-d_4: 225 (6), 197 (10), 195 (6), 181 (52), 153 (14), 149 (4), 119 (6), 105 (25), 103 (5), 90 (7), 89 (14), 88 (11), 77 (4), 74 (8), 62 (4), 61 (17), 60 (18), 58 (13), 46 (42), 45 (22), 43 (100), 42 (6), 33 (27), 32 (8), 30 (91), 29 (6). Ms of *dl*-(**7**)-d_4: 225 (3), 197 (12), 181 (31), 153 (18), 119 (4), 106 (3), 105 (20), 103 (5), 90 (5), 89 (12), 88 (8), 77 (4), 74 (7), 62 (4), 61 (15), 60 (15), 58 (12), 56 (3), 46 (35), 45 (18), 44 (23), 43 (100), 42 (6), 33 (24), 32 (10), 30 (82), 29 (5). All *m/z* values of 3% or more of (**7**) and (**7**)-d_4 isomers are shown above *m/z* 29.

For all 1:1 stoichiometry reactions, the six-membered ring acetal byproduct (2-methyl-5,5-dinitro-1,3-dioxacyclohexane) was formed in ≈ 16-19% relative abundance as determined by ^{1}H nmr integration of quartet patterns (Figure 5d). Gc/Ms analysis (Hewlett Packard 5985) indicated an 18.5% relative abundance of this byproduct (**9**); Ms of byproduct (**9**) [*m/z* (%)]: M^+ 191 (4), 177 (52), 102 (15), 101 (20), 99 (6), 85 (12), 74 (8), 71 (6), 60 (4), 59 (11), 58 (6), 57 (17), 56 (13), 55 (11), 54 (5), 46 (10), 45 (40), 44 (14), 43 (100), 42 (10), 40 (3), 39 (5), 31 (19), 30 (89), 29 (26); Ms of byproduct (**9**)-d_4: M^+ 195 (4), 181 (50), 106 (10), 105 (20), 103 (7), 89 (10), 78 (4), 74 (5), 62 (4), 61 (16), 60 (14), 58 (15), 56 (3), 46 (39), 45 (3), 44 (18), 43 (82), 42 (6), 33 (26), 32 (9), 30 (100). All *m/z* values of 3% or more of (**9**) and (**9**)-d_4 are shown above *m/z* 29.

2,2-Dinitropropane-1,3-diol (Compound 5).

The syntheses of (**5**) and its 2,2-dinitropropane-1,3-diol-1,1,3,3-d_4 analogue, (**5**)-d_4, are described in previous literature.[13] Ms of reactant (**5**) [*m/z* (%)]: M+1 167 (2), 102 (3), 74 (12), 73 (9), 72 (3), 57 (3), 56 (10), 55 (11), 54 (3), 48 (3), 47 (3), 46 (19), 45 (16), 44 (28), 43 (14), 42 (9), 31 (65), 30 (100), 29 (46); Ms of reactant (**5**)-d_4: M+1 171 (1), 78 (4), 77 (11), 60 (4), 59 (4), 58 (11), 57 (3), 56 (3), 49 (13), 48 (6), 46 (36), 45 (16), 44 (13), 43 (3), 42 (3), 34 (3), 33 (57), 32 (13), 31 (4), 30 (100), 29 (8). All *m/z* values of 3% or more of (**5**) and (**5**)-d_4 are shown above *m/z* 29.

1,3-Di-*tert*-butyl-5,5-dinitrohexahydropyrimidine (Compound 10).

The syntheses of this heterocycle (**10**) and its perdeuterio analogue, (**10**)-d_6, are described in previous literature.[13] Ms of compound (**10**) [*m/z* (%)]: M^+ 288 (10), 287 (53), 273 (5), 242 (9), 241 (12), 231 (7), 225 (5), 224 (28), 218 (4), 217 (32), 195 (4), 175 (18), 171 (8), 170 (4), 168 (6), 157 (13), 144 (6), 143 (72), 141 (8), 140 (5), 139 (6), 130 (10), 129 (9), 125 (4), 115 (21), 113 (6), 112 (20), 101 (19), 99 (6), 97 (4), 96 (10), 95 (5), 86 (33), 85 (6), 84 (7), 83 (20), 82 (8), 81 (6), 80 (4), 70 (28), 69 (4), 68 (5), 67 (4), 58 (13), 57 (100), 56 (14), 55 (12), 54 (7), 43 (5), 42 (16), 41 (43), 40 (3), 39 (11), 32 (4), 30 (16), 29 (22); Ms of compound (**10**)-d_6: M^+ 292 (18), 279 (5), 248 (4), 246 (9), 236 (4), 228 (6), 223 (23), 180 (6), 177 (7), 161 (4), 148 (4), 147 (32), 144 (5), 136 (4), 121 (11), 116 (6), 105 (5), 100 (4), 90 (5), 89 (27), 88 (10), 85 (3), 74 (3), 73 (5),

72 (25), 62 (3), 61 (3), 60 (6), 59 (5), 58 (12), 57 (100), 56 (6), 55 (5), 46 (13), 44 (5), 43 (4), 42 (8), 41 (42), 39 (8), 30 (7), 29 (12). All *m/z* values of 3% or more of (**10**) and (**10**)-d_6 are shown above *m/z* 29.

ACKNOWLEDGEMENTS

The authors are grateful to Dr Lee D. Smithson, AF Materials Laboratory, for obtaining the high resolution mass spectra used in this study, to Dr E. Dan Loughran, Los Alamos National Laboratory, and to Dr Thomas O. Tiernan, Wright State University, for confirmatory mass spectra analyses. Dr Michael B. Coolidge (FJSRL), Dr Christopher Adams, Dr Trevor Griffith, and Dr Norman Heimer provided useful technical discussion, and Dr James J.P. Stewart constructive manuscript review. Ms Angela Domitrovich (FJSRL) prepared all chemical structure figures for publication. Mr Jack Greathouse (FJSRL) obtained 300 MHz nmr spectra. Mrs Doreen G. Bagley, and Mrs Sylvia Miles of FJSRL, and the USAF Academy's Directorate of Audiovisual Services supplied helpful assistance in preparing this camera-ready manuscript. The Air Force Office of Scientific Research through Dr Don L. Ball, Director of Chemistry and Materials Sciences, furnished necessary financial support.

REFERENCES AND NOTES

1. Present address: Lawrence Livermore National Laboratory, PO Box 808 (Code L-394), Livermore CA 94550 (USA).
2. Present address: Alliance Pharmaceutical Corp., 3040 Science Park Road, San Diego CA 92121 (USA).
3. Correspondence author. Address as of 1 July 1994: Department of Chemistry, Bldg 753, United States Military Academy, West Point NY 10996.
4. R.E. Cochoy, R.R. McGuire, and S.A. Shackelford, J. Org. Chem., 1990, 55, 1401.
5. S.A. Shackelford, R.R. McGuire, and R.E. Cochoy, J. Org. Chem., 1992, 57, 2950.
6. F.W. McLafferty "Interpretation of Mass Spectra", Third Edition, ed. by N. J. Turro, University Science Books, Mill Valley, CA, 1980, p. 121.

7. B. Simonot and G. Rousseau, J. Org. Chem., 1993, 58, 4; and L. Mandolini, Adv. Physical Org. Chem., 1986, 22, 1 cited therein.

8. R.B. Silverstein, G.C. Bassler, and T.C. Morrill, "Spectrometric Identification of Organic Compounds", 4th Edition, John Wiley and Sons., New York, 1981, pp. 189-190, 206.

9. J. Collin, Bull. Soc. Roy. Sci. Liege, 1954, 23, 194.

10. R.T. Aplin, M. Fischer, D. Becher, H. Budzikiewicz, and C. Djerassi, J. Am. Chem. Soc., 1965, 87, 4888.

11. J.T. Larkins, F.E. Saalfeld, and L. Kaplan, Org. Mass Spectrom., 1969, 2, 213.

12. J. Yinon, "Mass Spectrometry Reviews", Vol 1, Wiley & Sons, New York, 1982, p. 257.

13. S.A. Shackelford, J. Labeled Compds. Radiopharm., 1991, 29, 1197.

14. J.T.B. Marshall and D.H. Williams, Tetrahedron, 1967, 23, 321.

15. H.B. Budzikiewicz, C. Djerassi, and D.H. Williams, "Mass Spectrometry of Organic Compounds", Holden-Day Inc., San Francisco, 1967, pp. 257-258.

16. S.R. Heller and G.W.A. Milne, "EPA/NIH Mass Spectral Data Base", Vol 1, US Government Printing Office, Washington DC 1978, p. 282.

17. Low resolution gc/ms analysis of compound (**7**) from Method 2 using the HP 5985 instrument gave no *m/z* 235 or 102 peak, while above *m/z* 31, *m/z* 177 was the third most prominent peak behind the base peak (*m/z*=43) and *m/z* 45.

18. Divinyl ether is no longer available from this source. Later quantities were purchased from Marshallton Research Laboratory, PO Box 11646, Winston-Salem NC 27106; however, recent inquiries reveal this source too no longer supplies this compound.

19. Divinyl ether contains a small amount of ethanol as a stabilizer and can become enriched with it upon long term storage; in this case, distillation over calcium hydride powder lowers the ethanol content to *ca.* 4 percent.

Received, 3rd June, 1991